

Supplementary information

A long-term stable paper-based glucose sensor using a glucose oxidase-loaded, Mn₂BPMP-conjugated nanocarrier with a smartphone readout

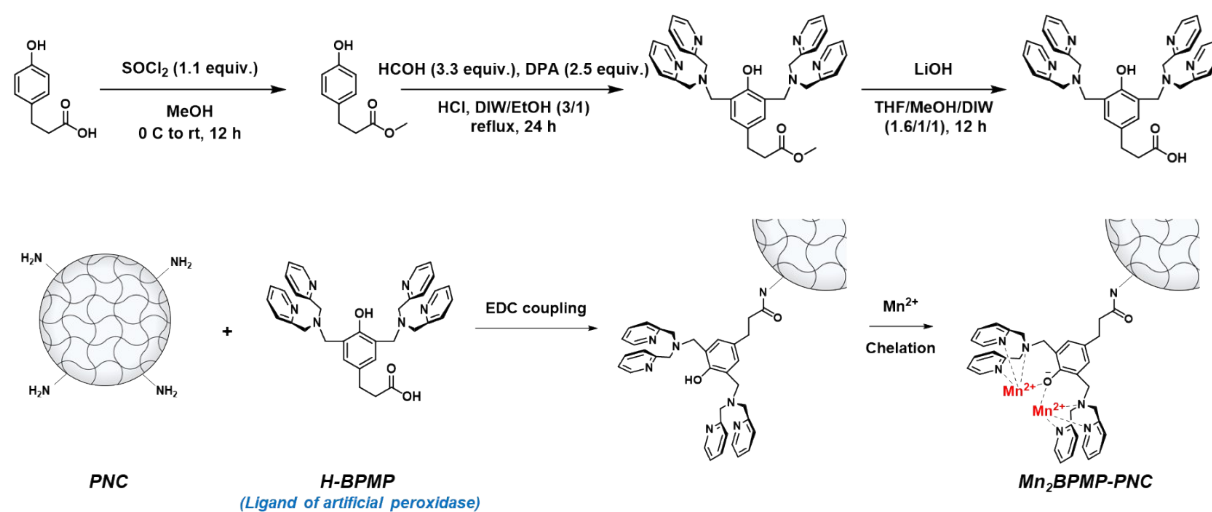
Soyeon Yoo,^{†a} Kiyoon Min,^{†b} Giyoong Tae*^b and Min Su Han*^a

^aDepartment of Chemistry, Gwangju Institute of Science and Technology (GIST), Gwangju 61005, Republic of Korea

^bSchool of Materials Science and Engineering, Gwangju Institute of Science and Technology (GIST), Gwangju 61005, Republic of Korea

* Corresponding author. E-mail: gytae@gist.ac.kr (G. Tae), happyhan@gist.ac.kr (M. S. Han)

Synthesis of Mn₂BPMP-PNC



Scheme S1. Synthesis scheme for Mn₂BPMP-PNC.

Synthesis of methyl 3-(4-hydroxyphenyl) propanoate¹

3-(4-hydroxyphenyl)propanoic acid (6.0 mmol, 1.0 g) was dissolved in 40 mL of methanol (MeOH) in an ice bath. Thionyl chloride (6.6 mmol, 0.5 mL) was slowly added dropwise to the solution and stirred at room temperature for 12 h. The solvent and residual thionyl chloride were subsequently evaporated under reduced pressure. The mixture was purified via column chromatography (ethyl acetate:hexane = 1:1) to yield a pale-yellow oil (1.1 g, yield 99.5%). ¹H-NMR (400 MHz, chloroform-D) δ 7.04 (d, *J* = 8.5 Hz, 2H), 6.75 (d, *J* = 8.5 Hz, 2H), 5.72 (s, 1H), 3.67 (s, 3H), 2.88 (t, *J* = 7.8 Hz, 2H), 2.61 (t, *J* = 7.8 Hz, 2H).

Synthesis of methyl 3-(3,5-bis((bis(pyridin-2-ylmethyl)amino)methyl)-4-hydroxyphenyl) propanoate (H-BPMP-CO₂Me)¹

Paraformaldehyde (3.3 mmol, 0.1 g) and di(2-picolyl)amine (2.5 mmol, 0.5 mL) were suspended in 12 mL of 75% aqueous ethanol. Methyl 3-(4-hydroxyphenyl)propanoate (1.0 mmol, 0.2 g) and 0.3 mL HCl (1.0 M) were added to the above solution and refluxed under stirring for 1 day. The solution was cooled to room temperature, neutralized with a saturated sodium carbonate solution, and extracted with excess chloroform. The organic layer was then collected, dried over sodium sulfate, and concentrated under reduced pressure. The mixture was purified via column chromatography (CHCl₃:MeOH = 20:1) to yield a pale-yellow solid (0.5 g, yield 86.2%). ¹H-NMR (400 MHz, chloroform-D) δ 10.91 (s, 1H), 8.54-8.46 (m, 5H), 7.58 (td, *J* = 7.6, 1.5 Hz, 4H), 7.47 (d, *J* = 7.6 Hz, 4H), 7.14-7.07 (m, 4H), 7.01 (s, 2H), 3.84 (s, 8H), 3.80-3.73 (4H), 3.63-3.58 (3H), 2.82 (t, *J* = 7.9 Hz, 2H), 2.54 (t, *J* = 7.9 Hz, 2H).

Synthesis of 3-(3,5-bis((bis(pyridin-2-ylmethyl)amino)methyl)-4-hydroxyphenyl) propanoic acid (H-BPMP-COOH)¹

H-BPMP-CO₂Me (1.0 mmol, 0.6 g) was dissolved in 130 mL of tetrahydrofuran/MeOH (1.6:1). Afterwards, 50 mL of LiOH solution (2.0 M) was added and the mixture was stirred for 12 h. Excess chloroform was then added to the solution and the pH was adjusted to 5–6 using a HCl solution (aq. 2 N). The organic layer was collected, washed with brine, dried over sodium

sulfate, and concentrated under reduced pressure to give H-BPMP-COOH (0.6 g, yield 97.0%). δ 8.52 (d, $J = 4.3$ Hz, 17H), 7.60 (td, $J = 7.6, 1.2$ Hz, 16H), 7.47 (d, $J = 7.9$ Hz, 16H), 7.14 (dd, $J = 7.3, 5.2$ Hz, 16H), 7.09 (s, 8H), 3.97 (s, 30H), 3.88 (s, 16H), 2.88 (t, $J = 7.2$ Hz, 8H), 2.65-2.55 (8H).

Synthesis of PNC²

Pluronic F127 (PF127) was diacrylated using acryloyl chloride and TEA in toluene, resulting in >95% degree of substitution. Methacrylated chitosan was obtained by reacting chitosan with glycidyl methacrylate. The degree of methacrylation was ~15% of the amine group of chitosan. Subsequently, an aqueous solution containing 0.77 wt% diacrylated PF127, 0.14 wt% of methacrylated chitosan, and Irgacure 2959 (0.05 wt%) as a photo-initiator was irradiated with 365 nm UV light at 1.3 mW/cm² using a UV lamp (VL-4.LC, 8 W, Viber Lourmat, France) for 15 min to induce photo-crosslinking. The crosslinked PNC was dialyzed against deionized water (DIW) using a 50 kDa dialysis membrane bag for 2 days for purification.

Synthesis of Mn₂BPMP-PNC

H-BPMP-COOH (44.6 μ mol, 26.3 mg), N-(3-dimethylaminopropyl)-N'-ethylcarbodiimide hydrochloride (EDCI; 22.3 μ mol, 42.8 g), and N-hydroxysuccinimide (NHS; 22.3 μ mol, 25.7 g) were dissolved in 20 mL of acetonitrile (ACN), and the solution was stirred for 2 h. After PNC (0.1 g) in 50 mL of DIW was added dropwise to the above solution, the mixture was stirred for 24 h. The solution was subsequently dialyzed in a 20% ACN aqueous solution for two days and an aqueous solution for 1 day. The H-BPMP-PNC (0.1 g) was obtained by lyophilization. Afterwards, Mn₂BPMP-PNC was prepared by chelating 2 equivalents of Mn(ClO₄)₂ with respect to BPMP in H-BPMP-PNC for 15 min.

Glucose assay in solution

Optimization of the GOx loading ratio to Mn₂BPMP-PNC

GOx at various concentrations (from 0 to 10 wt%) was loaded into Mn₂BPMP-PNC (2.7 mg/mL). Glucose (1 mM) was added to the buffer solutions (phosphate, 20 mM, pH 7.0) containing GOx-loaded Mn₂BPMP-PNC (2 μM) and ABTS (2 mM). The absorbance of the solutions at 417 nm was recorded at 30 s intervals for 10 min.

Glucose titration using Mn₂BPMP-PNC in solution

Glucose at various concentrations (0 to 1.5 mM) was added to a buffer solution (phosphate, 20 mM, pH 7.0) containing GOx (10 wt%)-loaded Mn₂BPMP-PNC (2 μM) and ABTS (2 mM). The absorbance of the solutions at 417 nm was monitored at 30 s intervals for 10 min. Similarly, glucose at various concentrations (0 to 1.5 mM) was added to the buffer solution (phosphate, 20 mM, pH 7.0, ACN 1%) containing Mn₂BPMP (2 μM), GOx (10 wt%) and ABTS (2 mM). The absorbance of the solutions at 417 nm was monitored at 30 s intervals for 10 min.

Analysis of substrate selectivity for Mn₂BPMP-PNC in solution

Various saccharides (galactose, fructose, maltose, lactose, sucrose; 10 mM, and glucose; 1 mM) were added to a buffer solution (phosphate, 20 mM, pH 7.0) containing GOx (10 wt%)-loaded Mn₂BPMP-PNC (2 μM) and ABTS (2 mM). Absorbance of the solutions at 417 nm was monitored at 30 s intervals for 10 min.

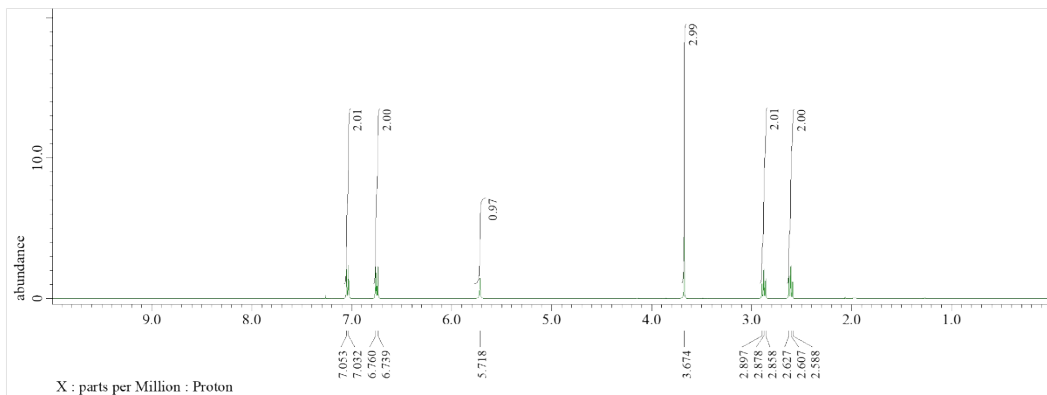


Fig. S1 ¹H NMR of methyl 3-(4-hydroxyphenyl) propanoate.

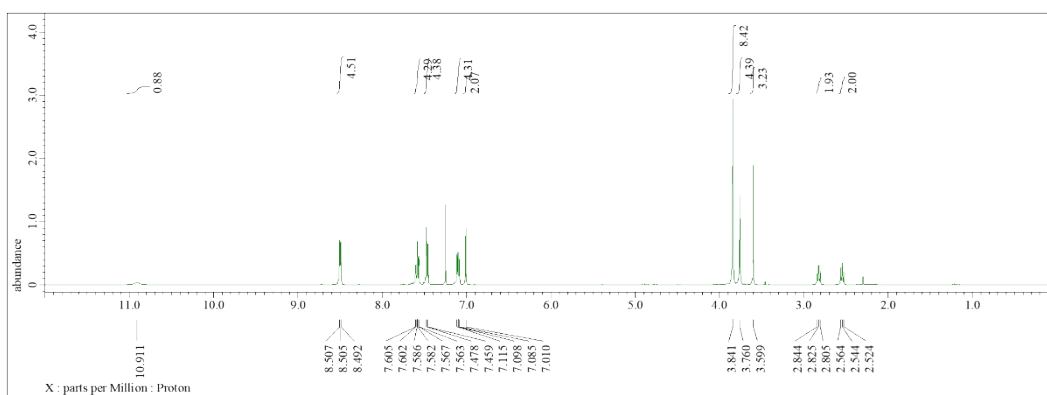


Fig. S2 ¹H NMR of H-BPMP-COOME.

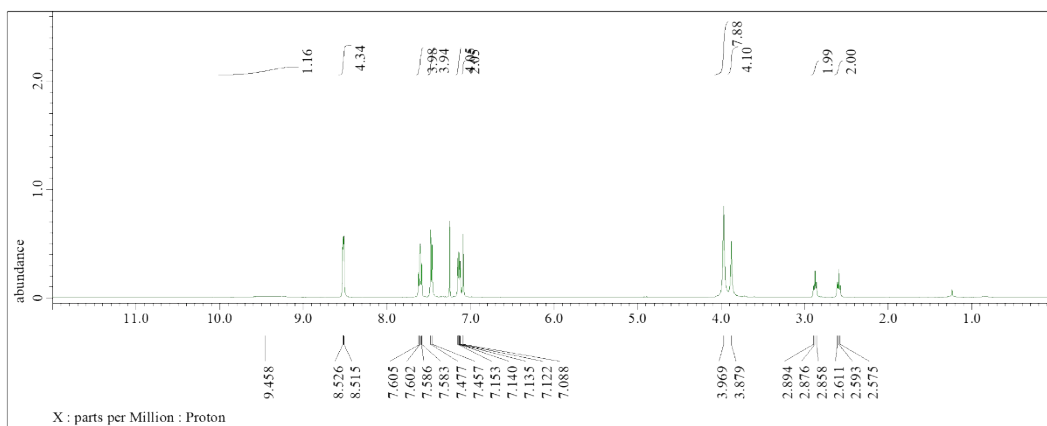


Fig. S3 ¹H NMR of H-BPMP-COOH.

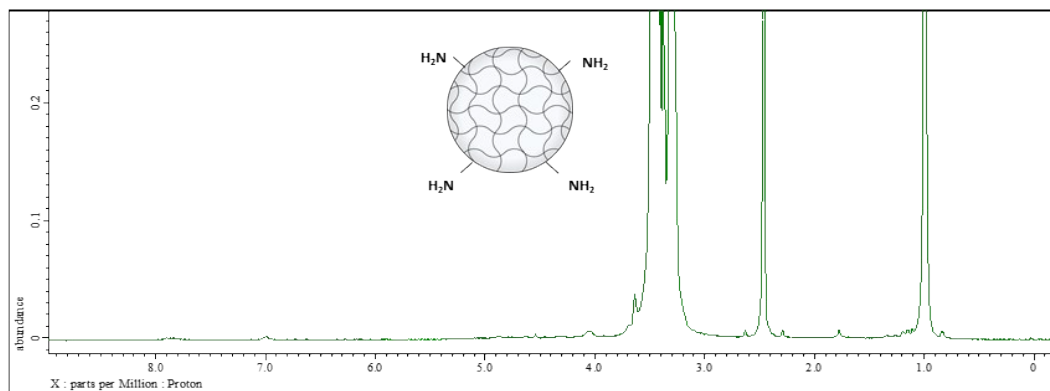


Fig. S4 ^1H NMR of PNC.

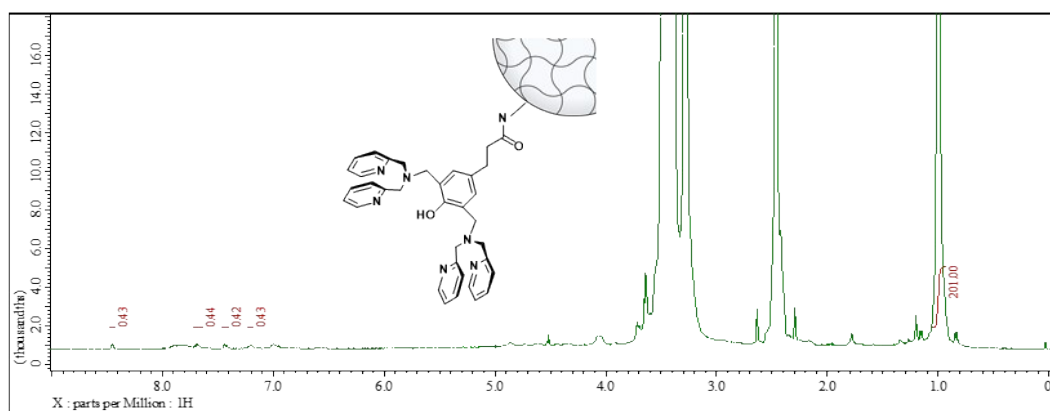


Fig. S5 ^1H NMR of H-BPMP-PNC.

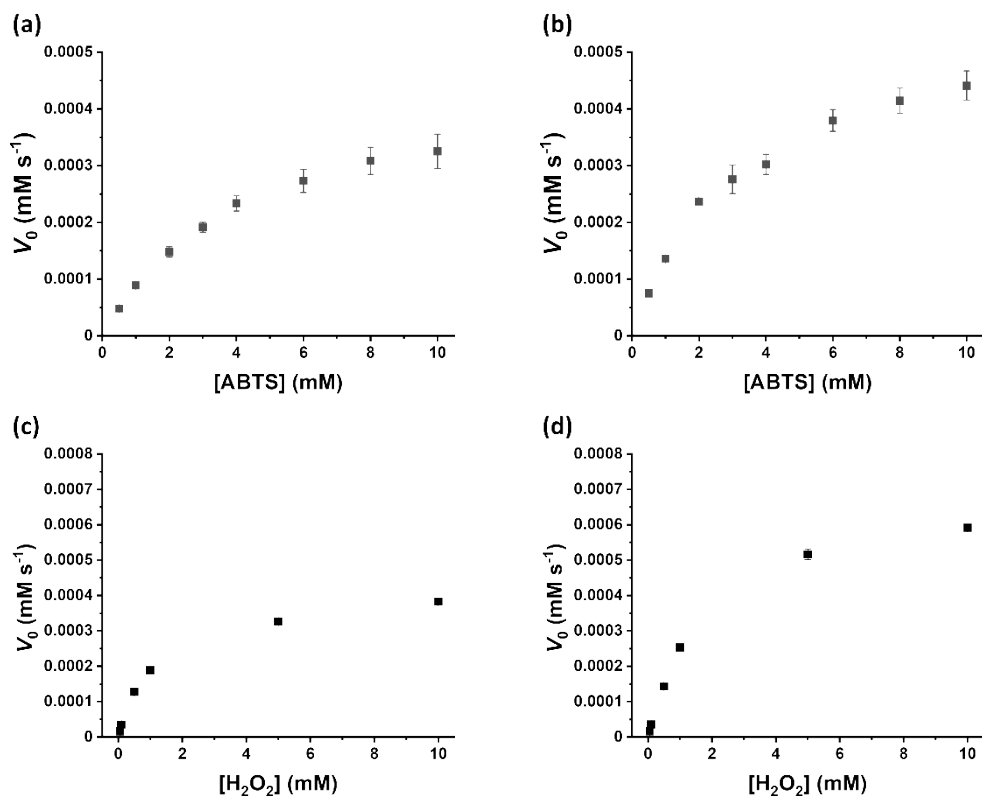


Fig. S6 Michaelis-Menten plots of the peroxidase-like activity of Mn₂BPMP (a, c) and Mn₂BPMP-PNC (b, d) versus the various concentrations of ABTS (a, b) or H₂O₂ (c, d) with a fixed concentration of the other substrate.

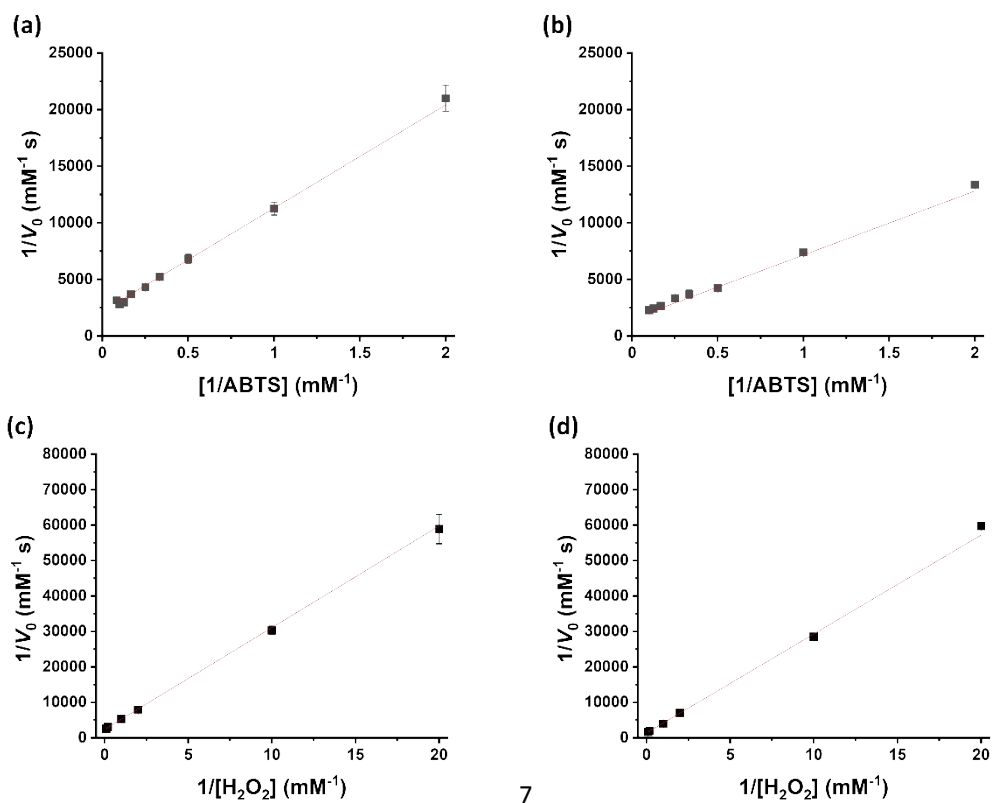


Fig. S7 Double reciprocal plots of the peroxidase-like activity of Mn₂BPMP (a, c) and Mn₂BPMP-PNC (b, d) versus concentration of ABTS (a, b) or H₂O₂ (c, d) with a fixed concentration of the other substrate.

Table S1 Comparison of the kinetic parameters obtained for HRP and other artificial peroxidases including Michaelis-Menten constants (K_m), maximum reaction rates (V_{max}), and catalytic constants (k_{cat})

| | Substrate | K_m (mM) | V_{max} (10^{-3} mM s^{-1}) | k_{cat} (s^{-1}) | Optimal pH | Reference |
|--|-------------------------------|---------------|--|---------------------------|------------|-----------|
| | ABTS | 0.472 | 55.0×10^{-2} | 4.837×10^3 | | 3 |
| Horseradish peroxidase (HRP) | TMB | 0.434 | 10.0×10^{-2} | 4.00×10^3 | 4.5 | 4 |
| | H ₂ O ₂ | 3.70 | 8.71×10^{-2} | 3.48×10^3 | | |
| Fe ₃ O ₄ nanoparticles | TMB | 0.098 | 3.44×10^{-2} | 3.02×10^4 | 3.5 - 4.5 | 4 |
| | H ₂ O ₂ | 154 | 9.78×10^{-2} | 8.58×10^4 | | |
| Gold nanoclusters | TMB | 3.59 | 8.61×10^{-3} | 2.87×10^{-3} | 3.0 - 4.0 | 5 |
| | H ₂ O ₂ | 16.71 | 13.02×10^{-3} | 4.34×10^{-3} | | |
| Co ₃ O ₄ nanoparticles | TMB | 0.037 | 6.27×10^{-2} | 1.83×10^2 | 5.0 | 6 |
| | H ₂ O ₂ | 140.07 | 1.21×10^{-1} | 3.53×10^2 | | |
| Single-layer Rh nanosheets | TMB | 0.264 | 12.56×10^{-2} | 8.2×10^4 | 4.0 | 7 |
| | H ₂ O ₂ | 4.51 | 68.09×10^{-2} | 44.5×10^4 | | |
| Cystein-MoS ₂ nanoflakes | ABTS | 0.15 | 1.61×10^{-1} | 0.64×10^4 | 4.0 | 8 |
| | H ₂ O ₂ | 8.06 | 9.92×10^{-1} | 3.97×10^4 | | |
| Cubic boron nitride | TMB | 0.157 | 18.54×10^{-2} | 5.98×10^4 | 4.0 | 9 |
| | H ₂ O ₂ | 10.88 | 10.69×10^{-2} | 3.45×10^4 | | |
| Fluorescein | TMB | 1.31 | 0.418×10^{-2} | 4.18×10^{-5} | 3.0 | 10 |
| | H ₂ O ₂ | 1.11 | 0.438×10^{-2} | 4.38×10^{-5} | | |
| Guanosine triphosphate | TMB | 2.93 | 9.15×10^{-2} | 9.15×10^{-3} | 5.0 | 11 |
| | H ₂ O ₂ | 0.761 | 1.80×10^{-2} | 1.80×10^{-3} | | |

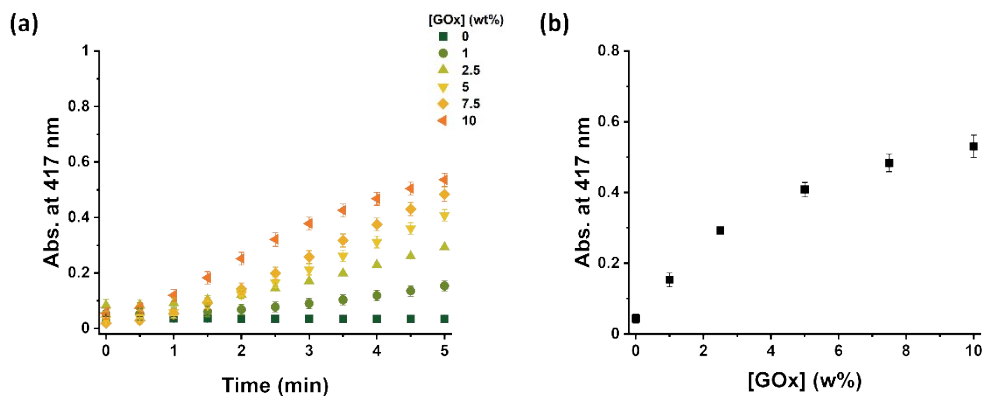


Fig. S8 (a) Absorbance changes of the ABTS/Mn₂BPMP-PNC/GOx system in the presence of glucose and various concentrations of GOx (from 0 to 10 wt% for Mn₂BPMP-PNC). (b) Plot of the absorbance at 417 nm *versus* GOx concentration at 5 min. [ABTS] = 2 mM, [Mn₂BPMP-PNC] = 2 μM, [glucose] = 1 mM in a buffer solution (phosphate, 20 mM, pH 7.0).

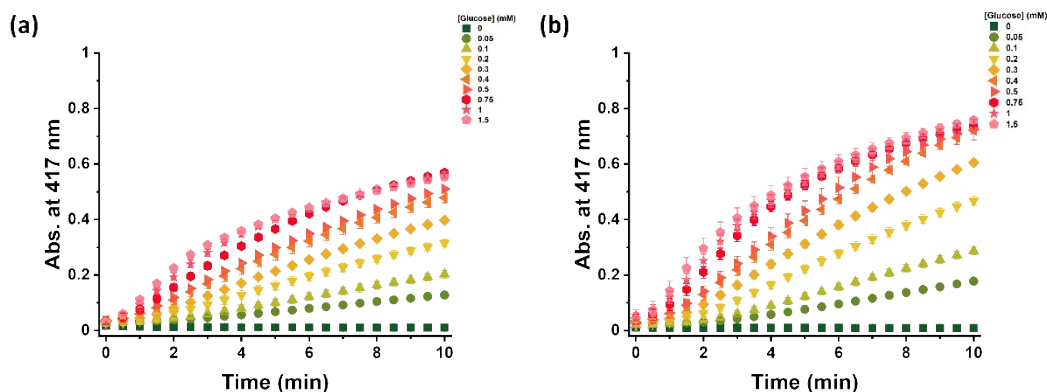


Fig. S9 Absorbance changes of (a) ABTS/ Mn_2BPMP /GOx system and (b) ABTS/ Mn_2BPMP -PNC/GOx system in the presence of various concentrations of glucose (from 0 to 1.5 mM). [ABTS] = 2 mM, [Mn_2BPMP -PNC] = [Mn_2BPMP] = 2 μ M, [GOx] = 10 wt% in a buffer solution (phosphate, 20 mM, pH 7.0).

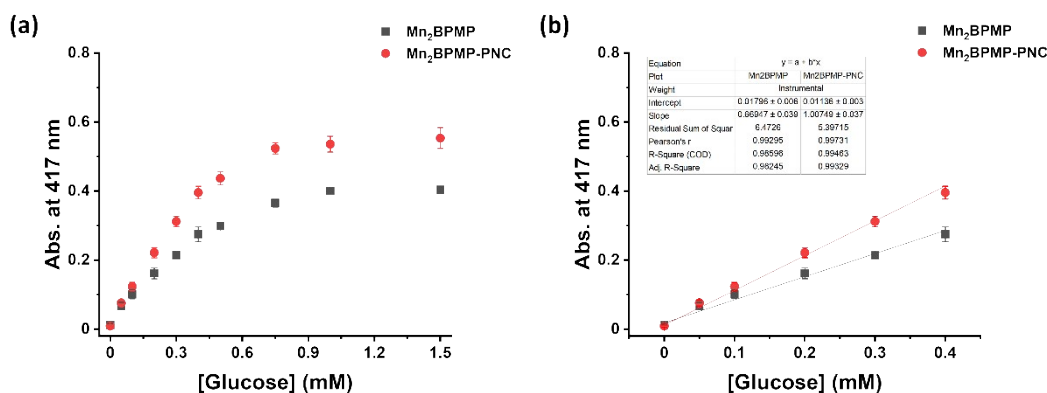


Fig. S10 (a) Absorbance at 417 nm for the ABTS/ Mn_2BPMP /GOx (black square) and ABTS/ Mn_2BPMP -PNC/GOx (red circle) systems at various glucose concentrations after 5 min. (b) Linear range of the plot of absorbance against the glucose concentrations. [ABTS] = 2 mM, [Mn_2BPMP -PNC] = [Mn_2BPMP] = 2 μ M, [GOx] = 10 wt% in a buffer solution (phosphate, 20 mM, pH 7.0).

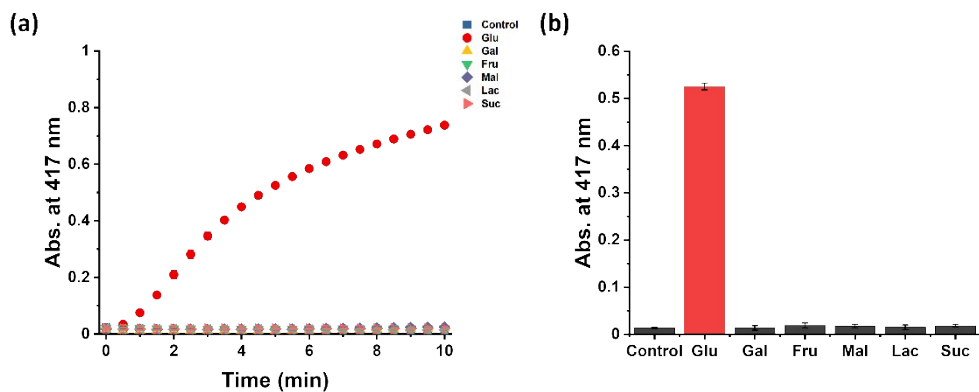


Fig. S11 (a) Absorbance change against time and (b) absorbance at 5 min of the ABTS/ Mn_2BPMP -PNC/GOx system in the presence of various saccharides. [ABTS] = 2 mM, [Mn_2BPMP -PNC] = 2 μ M, [GOx] = 10 wt%, [glucose] = 1 mM, [other saccharides] = 10 mM in a buffer solution (phosphate, 20 mM, pH 7.0).

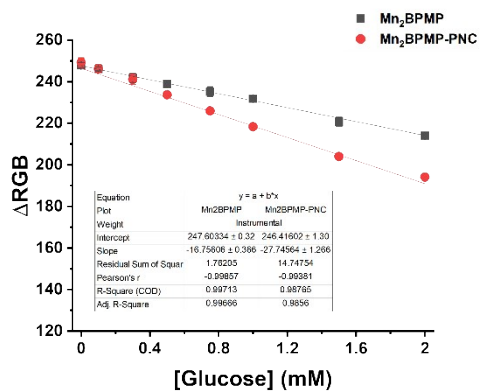


Fig. S12 Plot of the ΔRGB against the glucose concentrations in the PADs prepared using the ABTS/ Mn_2BPMP /GOx (black square) and ABTS/ Mn_2BPMP -PNC/GOx (red circle) systems.

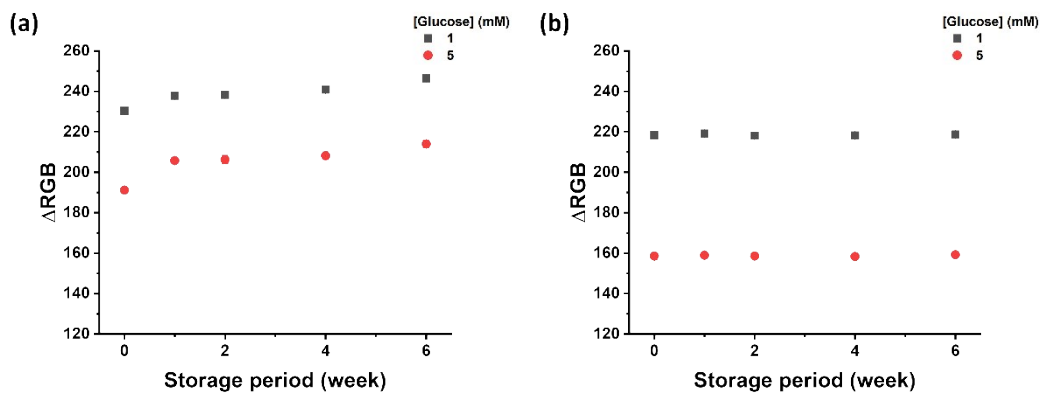


Fig. S13 Plot of the ΔRGB against the storage period in the PADs prepared with the (a) ABTS/ Mn_2BPMP /GOx and (b) ABTS/ Mn_2BPMP -PNC/GOx systems.

Table S2 Previous reports of paper-based glucose sensors

| Sensing system | Signal type | Readout | Detection range for glucose | Total sensing time and step | Real sample | Storage period and Temp. | Reference |
|--|--------------|---|-----------------------------|-----------------------------|-----------------|--------------------------|-----------|
| Chitosan supported GOx/HRP/TMB | Colorimetric | Scanner and Corel Photo-Paint™ software | 0.1 - 1 mM | 15 min, 1 step | Tear | | 12 |
| GOx/HRP-Cu ₃ (PO ₄) ₂ hybrid nanoflowers/TMB | Colorimetric | Digital camera and ImageJ software | 0.1 - 10 mM | 10 min, 1 step | Serum | 3 days, R.T. | 13 |
| Chitosan supported GOx/HRP/TMB | Colorimetric | Smartphone and ImageJ software | 0.02 - 4 mM | 10 min, 1 step | Serum and tear | | 14 |
| GOx/Au nanocluster/fluorescent graphene oxide | Fluorescent | Digital camera | 0.5 - 10 mM | 1h 10 min, 2 step | Serum | | 15 |
| Chitosan supported GOx/HRP/TBHBA | Colorimetric | Scanner and GIMP 2.8.22 software | 0 - 90 mgdL ⁻¹ | | Saliva | 10 days, - 4 °C | 16 |
| GOx/Antimony-doped tin oxide nanoparticles/TMB | Colorimetric | Smartphone and Image J software | 0.5 - 80 mM | 1h 6 min, 2 step | Glucose drink | | 17 |
| Chitosan supported GOx/HRP/TMB | Colorimetric | Smartphone and Color Name application | 50 - 600 μM | 6 min, 1 step | Sweat | | 18 |
| GOx/Co ₃ O ₄ -CeO ₂ nanosheets/TMB | Colorimetric | Smartphone and Color Picker application | 0.005 - 1.5 mM | 5 min, 1 step | Serum | 15 days, 4 °C | 19 |
| GOx/starch-iodine-gelatin | Colorimetric | Scanner and Adobe Photoshop CS 5 software | 0.5 - 5 mM | 15 min, 1 step | Serum | 6 week, - 20 °C | 20 |
| GOx/HRP/quantum dot | Fluorescent | Digital camera and ImageJ software | 1- 10 μM | 30 min, 1 step | Serum and urine | | 21 |
| Gox loaded Mn ₂ BPMP-PNC | Colorimetric | Smartphone and Color Grab application | 0.1-10 mM | 10 min, 1 step | Serum | 6 week, R.T. | This work |

HRP: horseradish peroxidase

TMB: 3,3,5,5-tetramethylbenzidine

TBHBA: 2,4,6-tribromo-3-hydroxyl benzoic acid

R.T.: room temperature

Reference

1. D. J. Oh, K. M. Kim and K. H. Ahn, *Chem. Asian J.*, 2011, **6**, 2034-2039.
2. J.-Y. Kim, W. I. Choi, Y. H. Kim, G. Tae, S.-Y. Lee, K. Kim and I. C. Kwon, *J. Controlled Release*, 2010, **147**, 109-117.
3. M. Drozd, M. Pietrzak, P. Parzuchowski, M. Mazurkiewicz-Pawlicka and E. Malinowska, *Nanotechnology*, 2015, **26**, 495101.
4. L. Gao, J. Zhuang, L. Nie, J. Zhang, Y. Zhang, N. Gu, T. Wang, J. Feng, D. Yang, S. Perrett and X. Yan, *Nat. Nanotechnol.*, 2007, **2**, 577-583.
5. L. Hu, H. Liao, L. Feng, M. Wang and W. Fu, *Anal. Chem.*, 2018, **90**, 6247-6252.
6. J. Mu, Y. Wang, M. Zhao and L. Zhang, *Chem. Commun.*, 2012, **48**, 2540-2542.
7. S. Cai, W. Xiao, H. Duan, X. Liang, C. Wang, R. Yang and Y. Li, *Nano Res.*, 2018, **11**, 6304-6315.
8. J. Yu, D. Ma, L. Mei, Q. Gao, W. Yin, X. Zhang, L. Yan, Z. Gu, X. Ma and Y. Zhao, *J. Mater. Chem. B*, 2018, **6**, 487-498.
9. T. M. Chen, J. Xiao and G. W. Yang, *RSC Adv.*, 2016, **6**, 70124-70132.
10. L. Liu, Y. Shi, Y. Yang, M. Li, Y. Long, Y. Huang and H. Zheng, *Chem. Commun.*, 2016, **52**, 13912-13915.
11. Y. Shi, M. Yang, L. Liu, Y. Pang, Y. Long and H. Zheng, *Sens. Actuator B-Chem.*, 2018, **275**, 43-49.
12. E. F. Gabriel, P. T. Garcia, F. M. Lopes and W. K. Coltro, *Micromachines*, 2017, **8**, 104.
13. X. Zhu, J. Huang, J. Liu, H. Zhang, J. Jiang and R. Yu, *Nanoscale*, 2017, **9**, 5658-5663.
14. X. Wang, F. Li, Z. Cai, K. Liu, J. Li, B. Zhang and J. He, *Anal. Bioanal. Chem.*, 2018, **410**, 2647-2655.
15. L. Su, L. Yang, Q. Sun, T. Zhao, B. Liu, C. Jiang and Z. Zhang, *New J. Chem.*, 2018, **42**, 6867-6872.
16. L. A. Santana-Jiménez, A. Márquez-Lucero, V. Osuna, I. Estrada-Moreno and R. B. Dominguez, *Sensors*, 2018, **18**, 1071.
17. Y. Li, J. Sun, W. Mao, S. Tang, K. Liu, T. Qi, H. Deng, W. Shen, L. Chen and L. Peng, *Microchim. Acta*, 2019, **186**, 403.
18. J. He, G. Xiao, X. Chen, Y. Qiao, D. Xu and Z. Lu, *RSC Adv.*, 2019, **9**, 23957-23963.
19. N. Alizadeh, A. Salimi and R. Hallaj, *Sens. Actuator B-Chem.*, 2019, **288**, 44-52.
20. M.-M. Liu, X. Lian, H. Liu, Z.-Z. Guo, H.-H. Huang, Y. Lei, H.-P. Peng, W. Chen, X.-H. Lin, A.-L. Liu and X.-H. Xia, *Talanta*, 2019, **200**, 511-517.
21. E. L. Rossini, M. I. Milani and H. R. Pezza, *Talanta*, 2019, **201**, 503-510.